

# Sex differences in monetary reward and punishment processing are associated with fast dynamics of dopamine synthesis

Andreas Hahn<sup>1\*</sup>, Murray B. Reed<sup>1</sup>, Verena Pichler<sup>2</sup>, Paul Michenthaler<sup>1</sup>, Lucas Rischka<sup>1</sup>, Godber M. Godbersen<sup>1</sup>, Wolfgang Wadsak<sup>2,3</sup>, Marcus Hacker<sup>2</sup>, Rupert Lanzenberger<sup>1\*</sup>

<sup>1</sup> *Department of Psychiatry and Psychotherapy, Medical University of Vienna, Austria*

<sup>2</sup> *Department of Biomedical Imaging and Image-guided Therapy, Division of Nuclear Medicine, Medical University of Vienna, Austria*

<sup>3</sup> *Center for Biomarker Research in Medicine (CBmed), Graz, Austria*

Word count	149	Abstract
	3390	Main section
	2435	Methods
Figures: 4, Tables: 0, References: 52		
Supplement: 1 figure		

\* **Correspondence to:** Andreas Hahn, Prof. PD PhD MSc  
Email: [andreas.hahn@meduniwien.ac.at](mailto:andreas.hahn@meduniwien.ac.at)  
ORCID: 0000-0001-9727-7580

or

Rupert Lanzenberger, Prof. PD MD  
Email: [rupert.lanzenberger@meduniwien.ac.at](mailto:rupert.lanzenberger@meduniwien.ac.at)  
ORCID: 0000-0003-4641-9539

Department of Psychiatry and Psychotherapy  
Medical University of Vienna, Austria  
Waehringer Guertel 18-20, 1090 Vienna, Austria

## KEY WORDS

reward, functional PET (fPET), functional MRI (fMRI), dopamine, sex differences

## **ABSTRACT**

Women and men show different behavioral sensitivity to reward and punishment, however, in humans the underlying neurotransmitter action has not yet been identified. Based on functional PET, we introduce a novel approach to enable the investigation of rapid changes in dopamine neurotransmission during cognitive task performance. In men, monetary gain induced 78% increase in dopamine synthesis vs. 49% for loss, whereas women showed the reverse pattern. Behavioral modeling revealed a direct association of task-specific dopamine synthesis with reward sensitivity in men and punishment sensitivity in women. Since dopaminergic sex differences were not reflected in BOLD signal changes, we emphasize a careful interpretation of fMRI-based studies on reward. This may have important implications in psychiatric conditions with sex-specific prevalence rates, alterations in reward processing and dopamine signaling. The high temporal resolution and magnitude of task-specific changes make fPET a promising tool to investigate such neurotransmitter dynamics in health and disease.

## INTRODUCTION

The processing of reward and punishment represents an essential aspect of one's mental health as reflected in alterations of the reward system in several psychiatric disorders such as addictive, gambling and eating disorders as well as depression. These disorders also exhibit a pronounced difference in the prevalence rates between men and women, which seems to be related to the well-established sex difference in reward and punishment sensitivity [1, 2]. Numerous different testing schemes have shown that women are more sensitive to threats and punishment, thus aiming for risk minimization and harm avoidance, whereas men opt for high rewards in terms of money, status and competitive success irrespective of the associated risks [3]. This sex difference is in line with evolutionary, psychological and neurobiological theories [3], however, it is not fully understood how such a difference maps onto human brain function.

The prevailing approach to investigate the neural representation of a particular behavioral effect is functional magnetic resonance imaging (fMRI) with the monetary incentive delay (MID) task being the most widely employed paradigm to study reward and punishment processing [4]. The aim of this task is to maximize monetary gain and avoid loss by reacting as fast as possible to a target stimulus within a given time limit. Probing differences between monetary gain and loss consistently shows activation of the nucleus accumbens (NAcc) [4], the major part of the ventral striatum [5], which is a pivotal region of reward processing [6, 7]. However, fMRI results of this [4, 8] or other reward paradigms [9, 10] do not report any sex differences in NAcc neuronal activation during reward consumption. This is potentially related to the dependence of fMRI on blood flow, reflecting post-synaptic glutamate signaling [11] instead of mapping specific modulatory neurotransmitter action [12].

A crucial role for the processing of reward and punishment is based on dopamine. Animal research has demonstrated that processing of these two distinct conditions is encoded by separate neurons of the ventral tegmental area [13, 14], projecting to the ventral

striatum/NAcc. In humans endogenous dopamine release can only be assessed indirectly by using specific positron emission tomography (PET) radioligands, which compete with the endogenous neurotransmitter to bind at a target receptor. Although the competition model represents a thoroughly validated approach it includes two disadvantages for the investigation of human behavior. Cognitive tasks only yield a rather low signal change around 5-15% from baseline [15], even for a recently introduced advancement that offers high temporal resolution [16]. Furthermore, separate measurements are required when aiming for comparison against a control condition, which is however highly desirable to support the specificity of the observed task effects. As such, among those studies investigating dopamine release during monetary gain [17-20] only one also evaluated loss but without observing any significant difference between the two conditions [21]. Interestingly, none of these studies considered sex-differences in task-induced dopamine release, despite numerous reports of general differences between men and women regarding ventral tegmental area functioning [22], dopamine synthesis rates at baseline [23] and amphetamine-induced release [24, 25] (but see [26]).

We therefore hypothesize that the assessment of task-specific changes in NAcc dopamine signaling during reward and punishment will resolve the discrepancy between behavioral sex-differences and the lack thereof in fMRI-based neuronal activation. To achieve this aim we introduce a novel approach, which enables the assessment of rapid changes in dopamine synthesis rates during cognitive performance by extending the technique of functional PET (fPET) imaging [27, 28] to a neurotransmitter level. Here, task-induced functional dynamics of dopamine synthesis were used as index of dopamine neurotransmission, focusing on the NAcc due to its pivotal role in the processing of reward and punishment. Following an initial proof of concept experiment, we specifically aim to investigate sex differences in the processing of monetary gain and loss by combined modeling of behavioral data, dopamine signaling and neuronal activation.

## RESULTS

### *Synthesis model and proof of concept*

To assess task-relevant changes in dopamine signaling during cognitive performance we developed a novel approach, which is based on the dynamic regulation of neurotransmitter synthesis. As most neurotransmitters cannot pass the blood brain barrier, they are synthesized in the brain from precursor molecules. For dopamine, the main pathway is the conversion of L-tyrosine to L-3,4-dihydroxyphenylalanine (DOPA) via the enzyme tyrosine hydroxylase, and then to dopamine by aromatic amino acid decarboxylase (AADC). Crucially, these enzymes are subject to fast-acting regulatory mechanisms. Tyrosine hydroxylase and AADC activities increase with neuronal firing in order to refill the synaptic vesicles after stimulus-induced dopamine release with *de novo* synthesized neurotransmitter and are further regulated by activation or blockade of dopamine receptors [29-31]. Moreover, the radioligand 6-[<sup>18</sup>F]FDOPA can be incorporated into this synthesis chain, as it is a substrate for AADC, rapidly forming 6-[<sup>18</sup>F]F-dopamine. The radioligand is thus specific for the dopaminergic pathway [32, 33] and represents an established approximation for dopamine synthesis rates [34]. Taken together, these data suggest that stimulus-induced activation of dopamine synthesis is also reflected in a proportionally increased radioligand binding (Fig. 1a-b).

This hypothesis can be directly tested by the application of 6-[<sup>18</sup>F]FDOPA within the framework of functional PET imaging [27, 35]. Similar to fMRI, fPET employs cognitive paradigms in repeated periods of task performance, thereby enabling the assessment of task-induced changes of multiple conditions within a single measurement. The radioligand 6-[<sup>18</sup>F]FDOPA is particularly suited for this application, as a bolus + infusion protocol [28] further emphasizes its apparently irreversible binding characteristics [34, 36] (Suppl. Fig. S1b and e), which in turn allows to identify task-specific changes in dopamine synthesis with high temporal resolution.

To assess the feasibility of the proposed model an initial proof of concept (PoC) experiment was conducted. Two subjects underwent fPET imaging with the radioligand 6- $^{18}\text{F}$ FDOPA while performing the MID task (Suppl. Fig. S1a). The paradigm comprised 3 blocks of 5 min each and in-between baseline periods resulting in a total scan time of 50 min. Each block included 27 trials of monetary gain and loss with different amounts, presented randomly. Following the assessment of the individual reaction time, the time limit for a successful trial outcome was adapted during the task: after each success (failure) the time limit was decreased (increased), which maintained the average probability for gain and loss at approximately 0.5. Dopamine synthesis rates ( $K_i$ ) at rest and during task performance were separated with the general linear model and quantified using the Patlak plot (Suppl. Fig. S1c and e) [27]. In both subjects the MID task induced substantial changes in NAcc dopamine synthesis of 78.4% and 59.4% from baseline (Fig. 1c), supporting the feasibility of the approach to assess task-specific changes in dopamine neurotransmission.

#### *Behavioral sex differences in reward and punishment processing*

Since the PoC experiment combined monetary gain and loss within a task block, we specifically aimed to disentangle these two effects on a behavioral and neurobiological level. The task was extended to 4 blocks and each of them manipulated to enable the separate assessment of monetary gain and loss (Suppl. Fig. S1a). For 2 blocks each, the time limit for a successful trial outcome was increased (decreased) in the beginning and middle of the block, thereby increasing the probability for gain (loss). Still, the adaption of the time limit during the task ensured that subjects were not aware of the manipulation. Furthermore, the inclusion of 6 different monetary amounts ( $\pm 3$ ,  $\pm 1$ ,  $\pm 0.5$  €) in the task enabled us to model the association with individual reaction times.

To investigate sex differences in the processing of reward and punishment on a behavioral level, 36 healthy subjects (18 female) completed the manipulated MID task, which included data obtained during the fPET scan. Average gain and loss were significantly different from

zero for both groups (all  $t = 10.0$  to  $12.6$ ,  $p = 1.7 \times 10^{-8}$  to  $2 \times 10^{-9}$ , Fig. 2a), indicating a successful task manipulation. Women gained significantly more than men ( $5.63 \pm 2.40$  € vs.  $4.21 \pm 1.67$  €,  $t = 2.1$ ,  $p = 0.047$ ), but both groups showed similar loss ( $-5.33 \pm 1.85$  € vs.  $-5.51 \pm 1.86$  €,  $p = 0.8$ ).

The difference in monetary gain was also reflected in the normalized reaction times, with a main effect of sex ( $F_{(1,34)} = 6.9$ ,  $p = 0.013$ ) and amount ( $F_{(5,170)} = 4.4$ ,  $p = 0.0009$ ) as well as a trend for an interaction effect sex \* amount ( $F_{(5,170)} = 2.0$ ,  $p = 0.08$ ). Post-hoc t-test indicated that this seemed to be driven by the  $-3$  € condition with women showing a faster reaction than men ( $t = 2.0$ ,  $p = 0.049$ ).

We further aimed to model the behavioral response in more detail, as the relationship between reaction time and amount for each group. In men this was best described by a negative linear function (reaction time =  $-0.18 - 2.36 \times \text{amount}$ ,  $p_{\text{linear}} = 0.0012$ ,  $p_{\text{quadratic}} = 0.11$ ), with a faster reaction for higher monetary gains (Fig. 2b). In contrast, the association in women was characterized by an inverted u-shaped function (reaction time =  $4.31 - 0.95 \times \text{amount} - 1.16 \times \text{amount}^2$ ,  $p_{\text{linear}} = 0.2$ ,  $p_{\text{quadratic}} = 0.001$ ), with faster reaction times for high amounts of loss as compared to men.

Overall, the behavioral data confirms previously reported sex differences in the processing of reward and punishment. More precisely, it seems that the sensitivity for monetary gain increases as a function of the reward value for both sexes. However, women showed a markedly different behavior than men when confronted with potential monetary loss. Men seemed to ascribe little relevance to loss, whereas women employed a harm avoidance strategy with faster reaction for high amounts of loss, leading to an overall higher amount of earned money.

### *Functional dynamics in dopamine synthesis during gain and loss*

To assess reward-specific changes in dopamine synthesis, 16 of the above subjects also underwent fPET with the radioligand 6- $^{18}\text{F}$ FDOPA (7 female). The imaging procedure was identical to the PoC experiment, except that the manipulated MID version was carried out to

separate the effects of monetary reward and punishment and dopamine synthesis rates were weighted by task performance. The manipulated MID paradigm yielded increased dopamine synthesis rates in the NAcc during gain (men:  $77.6 \pm 32.9\%$  from baseline, women:  $51.2 \pm 16.5\%$ ) and loss (men:  $49.4 \pm 26.7\%$ , women:  $78.4 \pm 18.6$ , all  $t = 5.5$  to  $11.1$ , all  $p = 0.0001$  to  $0.0005$ , Fig. 3b). As a result, the direct comparison between the two conditions showed higher dopamine synthesis rates in men for gain vs. loss ( $28.2 \pm 42.6\%$ ,  $t = 2.0$ ,  $p=0.08$ ). Interestingly, the direction of this difference was reversed in women with higher dopamine synthesis during loss vs. gain ( $-27.3 \pm 17.2\%$ ,  $t = -4.2$ ,  $p = 0.01$ , Fig. 4a).

Proceeding from the distinct models to characterize the behavioral response of monetary gain and loss (Fig. 2b), we assessed the relationship between individual model parameters (linear and quadratic terms) and task-specific dopamine synthesis rates. We herein interpreted the linear (quadratic) term for men (women) as index for reward (punishment) sensitivity, i.e., the more negative the parameter, the faster the reaction time for high gain (loss). This resulted in a significant association in men between the linear term and NAcc dopamine synthesis during gain ( $n = 9$ ,  $\rho = -0.7$ ,  $p = 0.043$ , Fig. 3c). On the other hand, the quadratic term in women was positively associated with NAcc dopamine synthesis of gain vs. loss ( $n = 7$ ,  $\rho = 0.89$ ,  $p = 0.012$ , Fig. 3d). These findings demonstrate sex-specific differences in dopamine neurotransmission during monetary gain and loss and directly link these task changes to the corresponding behavioral sensitivity for reward and punishment.

#### *Sex differences in reward-specific dopamine synthesis but not neuronal activation*

Finally, NAcc dopamine synthesis rates between gain vs. loss were significantly higher for men than women ( $t = 3.2$ ,  $p = 0.006$ , Fig. 4a). This sex difference was similarly present when using a functional delineation of the NAcc [4] ( $t = 2.7$ ,  $p = 0.02$ ), for raw dopamine synthesis values (i.e., not % signal change from baseline,  $t = 3.3$ ,  $p = 0.005$ ) and without weighting by task performance ( $t = 3.0$ ,  $p = 0.01$ ). Furthermore, the sex difference was specific for the NAcc as exploratory analysis revealed similar dopamine synthesis rates for men and women in the caudate ( $p = 0.8$ ) and putamen ( $p = 0.2$ ).



For direct comparison we also assessed neuronal activation, where the same subjects as in the fPET experiment also underwent fMRI, carrying out the MID task in 2 runs of 8.2 min each. In line with previous reports [4] we observed robust neuronal activation in the NAcc for gain vs. loss in men and women ( $t = 5.5$  to  $6.9$ ,  $p = 0.0005$  to  $0.0006$ , Fig. 4b). As expected, there was however no significant sex difference in activation for the atlas-based ( $p = 0.4$ ) or the functional delineation of the NAcc ( $p = 0.3$ ).

## DISCUSSION

In this work we introduce a novel framework for the assessment of task-specific changes in dopamine neurotransmission, which is based on the dynamic regulation of neurotransmitter synthesis quantified by functional PET imaging. Processing of monetary gain and loss induced robust changes in dopamine signaling in the living human brain even for the direct comparison of these two conditions, demonstrating the high sensitivity and specificity of the approach. Crucially, task-induced changes in dopamine synthesis showed sex-specific differences in the opposite direction with higher synthesis rates in men for gain vs. loss but vice versa in women, directly reflecting behavioral sex differences in reward and punishment sensitivity. Since this sex difference was not present in a conventional assessment of neuronal activation, our findings have important implications for the interpretation of numerous fMRI-based studies on reward processing. This is also essential in various clinical populations, where sex-specific effects on the link between altered reward processing and dopamine signaling is not yet fully understood [37].

The current work provides a biological basis for the well-known behavioral differences in reward and punishment sensitivity between men and women [1, 3]. We hereby extend general sex differences of the dopamine system [23-25] specifically to the processing of gain and loss and directly link changes in dopamine neurotransmission with the behavioral response. This is also supported by pharmacological responses observed in animals and humans. For instance, male rats aim for large rewards independent of the risk, whereas females decrease such choices in order to avoid punishment. Crucially, this sex difference was even more pronounced by the dopamine releasing agent amphetamine, where females almost completely abolished the choice for risky rewards [38]. On the other hand, studies in humans have shown that men often opt for selfish rewards, but women take more prosocial choices. However, pharmacological blockade of dopamine D2/D3 receptors shifts these preferences and thereby eliminate the difference in prosocial choices between men and women [39]. Taken together, these findings suggest that sex differences in reward behavior

are substantially driven by dopamine neurotransmission. It is still worth to note that pharmacological challenges may represent an unspecific assessment of neurotransmitter action. The systemic manipulation affects the entire brain, possibly eliciting complex downstream effects, and the use of potent challenge agents may overshadow subtle physiological and behavioral differences. Therefore, our results provide novel evidence in this context through the direct and spatially targeted assessment of reward-specific dopamine signaling itself. This enabled us to disentangle the dopaminergic involvement in monetary gain and loss, which revealed opposing changes in synthesis rates between men and women.

In contrast, such an evaluation was not accessible by previous approaches (see introduction for PET findings on the competition model). This also includes reward-specific neuronal activation obtained with fMRI, which did not reveal any (and particularly not opposing) sex differences between gain and loss in this or previous studies [4, 8, 9]. fMRI as based on the BOLD signal is dependent on the link between neuronal activation and changes in hemodynamic factors such as blood flow, volume and oxygenation [12, 40]. Blood flow is locally controlled by the major neurotransmitter glutamate, and thus it is widely accepted that the BOLD signal mostly reflects postsynaptic glutamate signaling [11, 41]. Although monoamine neurotransmitters such as dopamine may also modulate blood flow [42], this does not seem to translate into corresponding fMRI signal changes, at least for the processing of monetary gain and loss using the widely employed MID task. It is well-acknowledge that previous work has indicated a relationship between dopamine release and fMRI [43, 44], but these were again based on pharmacological manipulations, which may not be directly comparable to more subtle cognitive effects (see above). Instead, it appears that during cognitive task performance the limited contribution of dopamine to the BOLD signal gets lost in major downstream effects of glutamate action [11] and blood flow. We speculate that the latter two are not sufficiently specific [12] to identify sex differences in neuronal activation during reward processing. This may have substantial implications for the

investigation of several brain disorders with dopamine dysfunction such as addiction, schizophrenia or depression, where fMRI represents one of the most widely used methods to assess pathological alterations of brain function. Our results suggest that BOLD signal alterations may not primarily reflect the underlying dopaminergic changes, especially when investigating the reward system in men and women. Further work is required to elucidate the exact difference that subtle cognitive and potent pharmacological stimulation exert on the relationship between BOLD imaging and dopamine signaling and if this extends beyond sex differences of reward processing.

Although not directly assessed, there are two essential lines of evidence which strongly support the concept that task-specific changes in the 6-[<sup>18</sup>F]FDOPA signal are related to dopamine release. As mentioned above, dopamine synthesis is subject to fast-acting regulatory mechanisms and is activated by neuronal firing to refill the synaptic vesicles [29-31]. Moreover, dopamine synthesis is also increased by the dopamine releasing agent amphetamine as demonstrated in rats [45] and monkeys using PET [46]. Notably, a previous study reported no relationship between dopamine synthesis and release [47]. This is however not in contrast to the above concept since their work only investigated synthesis rates at baseline without any task performance or manipulation. Thus, the proposed approach offers an alternative to the competition model as the crucial factor to identify task-specific changes is the incorporation of radioligands into the dynamic regulation of enzymes responsible for neurotransmitter synthesis (instead of direct competition between radioligand and endogenous neurotransmitter).

The different neurobiological basis of these two approaches (i.e., competition vs. synthesis model) seems to explain the marked signal changes observed during the reward task of 75% from baseline and 25% for the direct comparison of gain vs. loss. This underlines the high sensitivity of the technique but also a high specificity with the ability to separate subtle effects of behaviorally similar conditions. Furthermore, fPET allows to assess task-specific changes

of multiple conditions in a single within-scan design, thereby eliminating intrasubject variability related to differences in habituation, motivation or performance of repeated measurements. These advantages seem to translate into robust effects even with a low sample size, thereby mitigating the limitation of the current study that imaging was only performed in a subset of the cohort. Another limitation is that we used a literature-based instead of an individual correction for radioactive metabolites. Although this may indeed change the absolute values of dopamine synthesis to a certain extent it does not influence the reward-specific effects. Again, in a within-scan design any “global” parameter will affect baseline and task-specific synthesis rates in an equal manner and will thus cancel out when calculating percent signal change or differences between gain and loss. This applies for instance to radioactive metabolites as well as previously reported sex differences in dopamine synthesis at baseline [23].

To summarize, the current work provides a strong motivation for further investigations of functional neurotransmitter dynamics during cognitive processing. The framework of fPET imaging offers important advantages of high temporal resolution and magnitude of task-induced changes as well as the possibility to assess multiple task conditions in a single measurement. Future studies should aim for an in-depth evaluation of stimulus-dependent activation of dopamine synthesis, proceeding from previous findings which link neurotransmitter synthesis and release [45, 46]. Moreover, our results suggest that reward-specific neuronal activation should not unequivocally be interpreted as corresponding changes in dopamine signaling and that the investigation of sex differences in this context requires further attention. This may be of pivotal relevance for the assessment of psychiatric populations such as addictive and gambling disorders or depression, given the different prevalence rates in men and women as well as alterations in reward processing and dopamine signaling. The introduced approach enables to address important future questions of human cognition and to investigate if the observed reward- and sex-specific differences in

dopamine synthesis will translate to clinically relevant characteristics for patient diagnosis or treatment.

## **METHODS**

### *Participants*

In total, 38 healthy participants were recruited for this study. Two healthy subjects participated in the proof of concept experiment (age 19.8 and 20.8 years, both female). For the main study another 36 healthy participants underwent behavioral testing with the monetary incentive delay (MID) task ( $24.5 \pm 4.3$  years, 18 female). From this group a subset of 16 participants also completed functional positron emission tomography (fPET) and functional magnetic resonance imaging (fMRI) examinations ( $24.8 \pm 4.8$  years, 7 female). Men and women did not differ regarding their age in the full sample ( $n = 36$ ,  $p = 0.69$ ) or the subsample ( $n = 16$ ,  $p = 0.51$ ).

General health of all participants was ensured at the screening visit by an experienced psychiatrist as based on the subjects' medical history. Exclusion criteria were current and previous (12 months) somatic, neurological or psychiatric disorders, current and previous substance abuse or psychotropic medication.

For participants who underwent PET and MRI a more extensive medical examination was carried out, including blood tests, electrocardiography, neurological testing and the Structural Clinical Interview for DSM-IV. Additional exclusion criteria were contraindications for MRI scanning, previous study-related radiation exposure (10 years), pregnancy or breast feeding. Thus, female participants underwent a urine pregnancy test at the screening visit and before the PET and MRI scans.

After detailed explanation of the study protocol, all participants gave written informed consent. Participants were insured and reimbursed for their participation. The study was approved by the Ethics Committee (ethics number: 2259/2017) of the Medical University of Vienna and procedures were carried out in accordance with the Declaration of Helsinki.

### *Cognitive task*

To assess reward and punishment processing the monetary incentive delay (MID) task was used, where participants aim to maximize gain and avoid loss by fast reaction upon

presentation of a target stimulus. The MID task represents a well-established paradigm [4] to investigate reward processing and has also been used previously by our group [48]. Each trial started with the presentation of the potential gain or loss (e.g., +3€, -1€) for a variable duration of 3 - 5 s (0.5 s steps, uniformly distributed). After that the target stimulus (!) was shown and subjects were required to press a button as fast as possible. If the reaction was within a given time limit the amount was gained or loss was avoided. Otherwise, the amount was not gained or lost. Each button press was followed by immediate feedback (2 s), showing the amount gained or lost, the outcome of the reaction (in green for success, red for failure) and the current account sum. Trials were separated by a crosshair with a variable duration of 3 - 7 s (1 s steps, uniformly distributed). To maintain a high level of attention and to enable modeling of the behavioral response, 6 different amounts of money were used for the task (0.5, 1 and 3 € each for gain and loss, initial amount was 10 €). Furthermore, motivation of the participants was kept high by the instruction that the final amount was paid out in addition to a fixed reimbursement.

The crucial aspect of this paradigm is the time limit of the reaction for the button press, where we employed an adaptive algorithm. For fPET and behavioral testing the task was carried out in several blocks, thus, the initial time limit of each block was set to the median of the reaction times of the previous block. The time limit for the first block (and for fMRI) was determined as median of 8 trials taken right before the start of the experiment in the scanner. Second, the time limit for each of the different amounts was adaptively decreased (increased) within a task block by 50 ms if the reaction was fast enough (too slow). These settings maintain an average probability of approximately 0.5 to gain or lose a certain amount.

For the proof of concept (PoC) experiments, 3 task blocks of 5 min were carried out each with 27 trials (equal distribution of amounts presented in random order) without further manipulation of the reaction time limits (i.e., probability of 0.5 for gain and loss).



For the main study, 4 task blocks of 5 min were carried out in a similar manner, but the probability for monetary gain and loss was manipulated within each block by changing the reaction time limit. For each of the 2 blocks of monetary gain (loss), the initial time limits of all amounts were increased (decreased) by 50 ms. Furthermore, in the middle of each block the time limits were reset to the median of the preceding reaction times and again adding (subtracting) 25 ms. This enabled the separate assessment of gain and loss even within the lower temporal resolution of fPET. The two conditions were presented in alternating order with randomization of the starting condition. Of note, monetary “gain” in this setting combines actual gain with avoided loss, whereas “loss” represents actual loss and omitted gain. The requirement for such a design is however well supported by previous studies indicating that avoided loss represents a relative reward [49]. For the behavioral testing, participants completed the same task version as for fPET but outside the scanner. For the fMRI measurements the MID task was carried out in 2 runs of 8.2 min each. The manipulation of the time limits (i.e., probability for gain and loss) was similar to that of fPET, but the trial order was randomized to avoid blocks of continuous gain or loss since fMRI has a higher temporal resolution and allows to model each trial separately. Furthermore, a neutral condition was included where no money was at stake (0 €). For all task versions, participants were blind to the adaption and manipulation of the time limits. This was also ensured by the choice to control the probability for gain and loss via the time limit, since overruling the participant’s actual reaction time would be easily recognized.

### *Magnetic resonance imaging (MRI)*

MRI data was obtained on a 3 T Magnetom Prisma scanner (Siemens Healthineers). A structural MRI was acquired with a T1-weighted MPRAGE sequence (TE/TR = 2.29/2300 ms, voxel size = 0.94 mm isotropic, 5.3 min), which was used to exclude gross neurological abnormalities and for spatial normalization of PET data. fMRI data was acquired using an EPI sequence (TE/TR = 30/2050 ms, voxel size = 2.1 x 2.1 x 2.8 mm + 0.7 mm slice gap).

### *Positron emission tomography (PET)*

The radioligand was freshly prepared every day by Iason GmbH or BSM Diagnostica GmbH. One hour before start of the PET measurement, each participant received 150 mg carbidopa p.o. to block peripheral metabolism of the radioligand by aromatic amino acid decarboxylase [34]. PET imaging was carried out using an Advance PET scanner (GE Healthcare) similar to previously described procedure [27]. To minimize head movement each participant's head was placed in a cushioned polyurethane bowl with straps around the forehead. The paradigm was visualized on a common LCD screen and presented to the subjects by a mirror, which was placed in front of the participant's eyes using a custom-made wooden construction. Attenuation correction was performed for 5 min with retractable  $^{68}\text{Ge}$  rod sources, which also included the mirror construction. Dynamic PET acquisition in 3D-mode started with the intravenous bolus + infusion of the radioligand 6- $^{18}\text{F}$ FDOPA. The injected dose was 5.5 MBq/kg body weight and the measurement time was 50 min. To increase the signal to noise ratio, 20% of the dose was given as bolus for 1 min [28] and the remainder as constant infusion for the rest of the scan (89 kBq/kg/min) using a perfusion pump (Syramed  $\mu\text{SP6000}$ , Arcomed, Regensdorf, Switzerland). During the scan the MID task was carried out at 10 (except for the PoC experiments), 20, 30 and 40 min after start of the radioligand application, each lasting for 5 min. Otherwise, a crosshair was presented and subjects were instructed to keep their eyes open and avoid focusing on anything specific (in particular not the task). PET images were then reconstructed to frames of 43 s, yielding 70 frames in total and 7 frames for each task block.

### *Blood sampling*

Arterial blood samples were drawn from the radial artery. Automatic sampling was carried out for the first 5 min (4 ml/min, Allogg, Mariefred, Sweden). Manual samples were taken at 3, 4, 5, 16, 26, 36 and 46 min, i.e., at periods of task pauses. For the manually obtained samples, activity in whole blood and plasma (after centrifugation) were measured in a gamma counter (Wizward<sup>2</sup>, 3", Perkin Elmer). Automatic and manual samples were then combined, were the

first manual samples served for a measurement-specific calibration between the automated sampling system and the gamma counter. Plasma to whole blood ratio was linearly interpolated between the manually acquired samples. Correction for radioactive metabolites was based on previous literature, assuming that the only relevant metabolite is 3-O-methyl-6- $[^{18}\text{F}]$ FDOPA (3-OMFD) after carbidopa pretreatment [34, 36, 50]. Thus, the 3-OMFD fraction was extracted from previous studies [50, 51] and fitted with a single exponential function (Suppl. Fig. S1d). Since this represents the metabolite fraction after a bolus application, we adapted the function to the herein employed radioligand application protocol as the sum of an initial 20% bolus and proportionally lower boli administered every further minute (Suppl. Fig. S1d). The final arterial input function was then obtained by multiplication of the whole blood curve with the plasma to whole blood ratio and the parent fraction. We are aware that a literature-based metabolite correction may affect the individual estimates of dopamine synthesis rates. However, it equally affects task-specific changes thereof as they are acquired within the same measurement. Thus, the individual variation in metabolism will cancel out when calculating percent signal change from baseline and differences between task conditions (see also discussion section). Moreover, the bolus + infusion protocol resulted in a reduction of the 3-OMFD fraction by 51.4% (area under the curve), further minimizing the influence of radioactive metabolites.

#### *Quantification of dopamine synthesis rates*

Image preprocessing was done as described previously [28] using SPM12 and default parameters unless specified otherwise. PET images were corrected for head motion (quality = 1, registered to mean) and the resulting mean image was coregistered to the T1-weighted structural MRI. The structural scan was spatially normalized to MNI space and the resulting transformation matrices (coregistration and normalization) were applied to the dynamic PET images. Images were smoothed with an 8 mm Gaussian kernel, masked to include only gray matter voxels and a low-pass filter was applied with the cutoff frequency set to 2.5 min.

The general linear model was used to separate task effects from baseline synthesis (Suppl. Fig. S1c). This included one regressor for each task block (except for the PoC experiments where a single task regressor was used) with a slope of 1 kBq/frame, one representing baseline dopamine synthesis and one for head motion (first principal component of the six motion regressors). The baseline was defined as average time course of all gray matter voxels, excluding those activated in the corresponding fMRI acquisition (contrast success > failure,  $p < 0.001$  uncorrected) and those identified in a recent meta-analysis of the MID task (contrasts reward/loss anticipation and reward outcome) [4]. The Patlak plot was then applied to compute the net influx constant  $K_i$  as index of dopamine synthesis for baseline and task effects separately (Suppl. Fig. S1e). Task-specific percent signal change (PSC) from baseline was calculated as

$$PSC_{K_i} = K_{i_{\text{task}}} / K_{i_{\text{baseline}}} * 100 \quad (1)$$

The four task blocks were finally weighted according to task performance (actual gain/possible gain, similar for loss) and averaged to obtain task specific  $PSC_{K_i}$  for gain and loss. To assess the specificity of the findings, task-specific changes in dopamine synthesis rates were also calculated independently of baseline  $K_i$  values (i.e., not PSC) and without weighting by task performance.

### *Neuronal activation*

Task-induced neuronal activation was computed as described previously using SPM12 [48]. fMRI BOLD images were corrected for slice timing differences (reference: middle slice) and head motion (quality = 1, registered to mean), spatially normalized to MNI space and smoothed with an 8 mm Gaussian kernel. Neuronal activation was estimated across the two runs with the general linear model including one regressor for each cue (gain, loss, neutral), one for the target stimulus and one for each of the potential outcomes (gain, omitted gain, loss, avoided loss, neutral) as well as several nuisance regressors (motion, white matter, cerebrospinal fluid). To obtain an index of reward outcome [4] which is as similar to fPET as

possible, parameter estimates were combined as (gain + avoided loss) – (omitted gain + loss). Percent signal changes were computed as

$$PSC_{fMRI} = \beta_{task} / \beta_{baseline} * 100 * peak \quad (2)$$

with  $\beta_{baseline}$  and peak representing the constant and the peak value of the fMRI design matrix, respectively [52].

### *Statistical analysis*

The accumulated amount that was gained and lost during the corresponding task blocks of the MID were assessed with one sample t-tests against zero, whereas sex differences were computed by independent samples t-tests. Due to the adaptive nature of the MID task the reaction times were normalized to the mean by subtracting the average reaction time within each block. Differences in reaction times were evaluated by repeated measures ANOVA with the factors sex and amount. Post-hoc t-tests were used to assess sex differences for each amount. Furthermore, we modeled the relationship between reaction time and amount with a 2<sup>nd</sup> order polynomial function to estimate linear and nonlinear effects. This was done across the entire group (n = 36) to test for a general relationship. Subsequently, model parameters were also estimated individually for the fPET subjects (n = 16) to assess the correlation with task-specific changes in dopamine synthesis using Spearman's correlation (since n < 10 in each group for fPET).

For imaging parameters, the primary hypothesis concerned the NAcc due to its pivotal importance in reward processing [6, 7]. Therefore, regional values of  $PSC_{Ki}$  and  $PSC_{fMRI}$  were extracted for this region using the Harvard Oxford atlas as provided in FSL. For comparison, a functional definition of the NAcc was also employed (neuronal activation of reward outcome [4]), which comprised 2.55 cm<sup>3</sup> (in contrast to the NAcc of the Harvard-Oxford atlas with only 1.38 cm<sup>3</sup>). Task-specific changes in dopamine synthesis rates were evaluated by one sample t-tests against zero for gain and loss separately. Similarly, for  $PSC_{Ki}$  and  $PSC_{fMRI}$  the difference of gain vs. loss was calculated and assessed by one sample t-tests against zero (i.e., being identical to a paired samples t-tests). Finally, sex differences in  $PSC_{Ki}$  and

$PSC_{fMRI}$  were addressed with an independent samples t-test. All statistical tests were corrected for multiple comparisons with the Bonferroni-Holm procedure (e.g., when testing multiple conditions and/or groups) and the reported p-values have been adjusted accordingly.

## **ACKNOWLEDGEMENTS**

The authors are particularly grateful to S. Oldham and V. Lorenzetti for providing the meta-analysis maps of the monetary incentive delay task. We would like to thank P. Baldinger-Melich and A. Basaran for medical and measurement support as well as V. Ritter and the diploma students of the Neuroimaging Labs for subject recruitment and administrative support.

This research was supported by a grant from the Austrian Science Fund to A. Hahn (FWF KLI 610). L. Rischka is recipient of a DOC Fellowship of the Austrian Academy of Sciences at the Department of Psychiatry and Psychotherapy, Medical University of Vienna. The scientific project was performed with the support of the Medical Imaging Cluster of the Medical University of Vienna.

## **AUTHOR CONTRIBUTIONS**

Study design: A.H., W.W., M.H., R.L.

Data acquisition: M.B.R., L.R., A.H., V.P., P.M., G.M.G.

Data analysis: A.H., M.B.R., L.R.

Manuscript preparation: A.H., L.R., M.B.R., R.L.

All authors discussed the implications of the findings and approved the final version of the manuscript.

## **COMPETING INTERESTS**

W.W. declares to having received speaker honoraria from the GE Healthcare and research grants from Ipsen Pharma, Eckert-Ziegler AG, Scintomics, and ITG; and working as a part time employee of CBmed Ltd. (Center for Biomarker Research in Medicine, Graz, Austria). M.H. received consulting fees and/or honoraria from Bayer Healthcare BMS, Eli Lilly, EZAG, GE Healthcare, Ipsen, ITM, Janssen, Roche, and Siemens Healthineers. R.L. received travel

grants and/or conference speaker honoraria within the last three years from Bruker BioSpin MR, Heel, and support from Siemens Healthcare regarding clinical research using PET/MR. He is shareholder of BM Health GmbH since 2019. A.H., M.B.R., L.R. G.M.G, P.M. and V.P. report no conflict of interest in relation to this study.

## REFERENCES

1. Torrubia, R., et al., *The Sensitivity to Punishment and Sensitivity to Reward Questionnaire (SPSRQ) as a measure of Gray's anxiety and impulsivity dimensions*. Personality and Individual Differences, 2001. **31**(6): p. 837-862.
2. Eneva, K.T., et al., *Reward and punishment sensitivity and disordered eating behaviors in men and women*. J Eat Disord, 2017. **5**: p. 6.
3. Cross, C.P., L.T. Copping, and A. Campbell, *Sex differences in impulsivity: a meta-analysis*. Psychol Bull, 2011. **137**(1): p. 97-130.
4. Oldham, S., et al., *The anticipation and outcome phases of reward and loss processing: A neuroimaging meta-analysis of the monetary incentive delay task*. Hum Brain Mapp, 2018. **39**(8): p. 3398-3418.
5. Neto, L.L., et al., *The human nucleus accumbens: where is it? A stereotactic, anatomical and magnetic resonance imaging study*. Neuromodulation, 2008. **11**(1): p. 13-22.
6. Berridge, K.C. and M.L. Kringelbach, *Affective neuroscience of pleasure: reward in humans and animals*. Psychopharmacology (Berl), 2008. **199**(3): p. 457-80.
7. Haber, S.N. and B. Knutson, *The reward circuit: linking primate anatomy and human imaging*. Neuropsychopharmacology, 2010. **35**(1): p. 4-26.
8. Rademacher, L., et al., *Dissociation of neural networks for anticipation and consumption of monetary and social rewards*. Neuroimage, 2010. **49**(4): p. 3276-85.
9. Weafer, J., et al., *Neural correlates of inhibition and reward are negatively associated*. Neuroimage, 2019. **196**: p. 188-194.
10. van den Bos, R., J. Homberg, and L. de Visser, *A critical review of sex differences in decision-making tasks: focus on the Iowa Gambling Task*. Behav Brain Res, 2013. **238**: p. 95-108.
11. Attwell, D. and S.B. Laughlin, *An energy budget for signaling in the grey matter of the brain*. J Cereb Blood Flow Metab, 2001. **21**(10): p. 1133-45.
12. Heeger, D.J. and D. Ress, *What does fMRI tell us about neuronal activity?* Nat Rev Neurosci, 2002. **3**(2): p. 142-51.



13. Matsumoto, M. and O. Hikosaka, *Two types of dopamine neuron distinctly convey positive and negative motivational signals*. Nature, 2009. **459**(7248): p. 837-41.
14. Cohen, J.Y., et al., *Neuron-type-specific signals for reward and punishment in the ventral tegmental area*. Nature, 2012. **482**(7383): p. 85-8.
15. Egerton, A., et al., *The dopaminergic basis of human behaviors: A review of molecular imaging studies*. Neurosci Biobehav Rev, 2009. **33**(7): p. 1109-32.
16. Lippert, R.N., et al., *Time-dependent assessment of stimulus-evoked regional dopamine release*. Nat Commun, 2019. **10**(1): p. 336.
17. Schott, B.H., et al., *Mesolimbic functional magnetic resonance imaging activations during reward anticipation correlate with reward-related ventral striatal dopamine release*. J Neurosci, 2008. **28**(52): p. 14311-9.
18. Joutsa, J., et al., *Mesolimbic dopamine release is linked to symptom severity in pathological gambling*. Neuroimage, 2012. **60**(4): p. 1992-9.
19. Jonasson, L.S., et al., *Dopamine release in nucleus accumbens during rewarded task switching measured by [(1)(1)C]raclopride*. Neuroimage, 2014. **99**: p. 357-64.
20. Weiland, B.J., et al., *Relationship between impulsivity, prefrontal anticipatory activation, and striatal dopamine release during rewarded task performance*. Psychiatry Res, 2014. **223**(3): p. 244-52.
21. Pappata, S., et al., *In vivo detection of striatal dopamine release during reward: a PET study with [(11)C]raclopride and a single dynamic scan approach*. Neuroimage, 2002. **16**(4): p. 1015-27.
22. Gillies, G.E., et al., *Sex-dependent diversity in ventral tegmental dopaminergic neurons and developmental programming: A molecular, cellular and behavioral analysis*. Neuroscience, 2014. **282**: p. 69-85.
23. Laakso, A., et al., *Sex differences in striatal presynaptic dopamine synthesis capacity in healthy subjects*. Biol Psychiatry, 2002. **52**(7): p. 759-63.
24. Munro, C.A., et al., *Sex differences in striatal dopamine release in healthy adults*. Biol Psychiatry, 2006. **59**(10): p. 966-74.
25. Riccardi, P., et al., *Sex differences in amphetamine-induced displacement of [(18)F]fallypride in striatal and extrastriatal regions: a PET study*. Am J Psychiatry, 2006. **163**(9): p. 1639-41.
26. Smith, C.T., et al., *Lack of consistent sex differences in D-amphetamine-induced dopamine release measured with [(18)F]fallypride PET*. Psychopharmacology (Berl), 2019. **236**(2): p. 581-590.
27. Hahn, A., et al., *Quantification of Task-Specific Glucose Metabolism with Constant Infusion of 18F-FDG*. J Nucl Med, 2016. **57**(12): p. 1933-1940.
28. Rischka, L., et al., *Reduced task durations in functional PET imaging with [(18)F]FDG approaching that of functional MRI*. Neuroimage, 2018. **181**: p. 323-330.
29. Morgenroth, V.H., 3rd, M. Boadle-Biber, and R.H. Roth, *Tyrosine hydroxylase: activation by nerve stimulation*. Proc Natl Acad Sci U S A, 1974. **71**(11): p. 4283-7.

30. Neff, N.H. and M. Hadjiconstantinou, *Aromatic L-amino acid decarboxylase modulation and Parkinson's disease*. Prog Brain Res, 1995. **106**: p. 91-7.
31. Meiser, J., D. Weindl, and K. Hiller, *Complexity of dopamine metabolism*. Cell Commun Signal, 2013. **11**(1): p. 34.
32. Doudet, D.J., et al., *6-[F-18]fluoro-L-DOPA PET studies of the turnover of dopamine in MPTP-induced parkinsonism in monkeys*. Synapse, 1998. **29**(3): p. 225-232.
33. Rinne, J.O., et al., *[F-18]FDOPA and [F-18]CFT are both sensitive PET markers to detect presynaptic dopaminergic hypofunction in early Parkinson's disease*. Synapse, 2001. **40**(3): p. 193-200.
34. Cumming, P. and A. Gjedde, *Compartmental analysis of dopa decarboxylation in living brain from dynamic positron emission tomograms*. Synapse, 1998. **29**(1): p. 37-61.
35. Villien, M., et al., *Dynamic functional imaging of brain glucose utilization using fPET-FDG*. Neuroimage, 2014. **100**: p. 192-9.
36. Holden, J.E., et al., *Graphical analysis of 6-fluoro-L-dopa trapping: effect of inhibition of catechol-O-methyltransferase*. J Nucl Med, 1997. **38**(10): p. 1568-74.
37. Becker, J.B. and E. Chartoff, *Sex differences in neural mechanisms mediating reward and addiction*. Neuropsychopharmacology, 2019. **44**(1): p. 166-183.
38. Orsini, C.A., et al., *Sex differences in a rat model of risky decision making*. Behav Neurosci, 2016. **130**(1): p. 50-61.
39. Soutschek, A., et al., *The dopaminergic reward system underpins gender differences in social preferences*. Nat Hum Behav, 2017. **1**(11): p. 819-827.
40. Norris, D.G., *Principles of magnetic resonance assessment of brain function*. J Magn Reson Imaging, 2006. **23**(6): p. 794-807.
41. Logothetis, N.K., et al., *Neurophysiological investigation of the basis of the fMRI signal*. Nature, 2001. **412**(6843): p. 150-7.
42. Krimer, L.S., et al., *Dopaminergic regulation of cerebral cortical microcirculation*. Nat Neurosci, 1998. **1**(4): p. 286-9.
43. Knutson, B. and S.E. Gibbs, *Linking nucleus accumbens dopamine and blood oxygenation*. Psychopharmacology (Berl), 2007. **191**(3): p. 813-22.
44. Sander, C.Y., et al., *Neurovascular coupling to D2/D3 dopamine receptor occupancy using simultaneous PET/functional MRI*. Proc Natl Acad Sci U S A, 2013. **110**(27): p. 11169-74.
45. Kehr, W., W. Speckenbach, and R. Zimmermann, *Interaction of haloperidol and gamma-butyrolactone with (+)-amphetamine-induced changes in monoamine synthesis and metabolism in rat brain*. J Neural Transm, 1977. **40**(2): p. 129-47.
46. Hartvig, P., et al., *Amphetamine effects on dopamine release and synthesis rate studied in the Rhesus monkey brain by positron emission tomography*. J Neural Transm (Vienna), 1997. **104**(4-5): p. 329-39.

47. Berry, A.S., et al., *Dopamine Synthesis Capacity is Associated with D2/3 Receptor Binding but Not Dopamine Release*. *Neuropsychopharmacology*, 2018. **43**(6): p. 1201-1211.
48. Pfabigan, D.M., et al., *P300 amplitude variation is related to ventral striatum BOLD response during gain and loss anticipation: an EEG and fMRI experiment*. *Neuroimage*, 2014. **96**: p. 12-21.
49. Pessiglione, M., et al., *Dopamine-dependent prediction errors underpin reward-seeking behaviour in humans*. *Nature*, 2006. **442**(7106): p. 1042-5.
50. Huang, S.C., et al., *Kinetics and modeling of L-6-[18F]fluoro-dopa in human positron emission tomographic studies*. *J Cereb Blood Flow Metab*, 1991. **11**(6): p. 898-913.
51. Doudet, D.J., et al., *Evaluation of dopaminergic presynaptic integrity: 6-[18F]fluoro-L-dopa versus 6-[18F]fluoro-L-m-tyrosine*. *J Cereb Blood Flow Metab*, 1999. **19**(3): p. 278-87.
52. Luo, W.L. and T.E. Nichols, *Diagnosis and exploration of massively univariate neuroimaging models*. *Neuroimage*, 2003. **19**(3): p. 1014-32.

## FIGURES

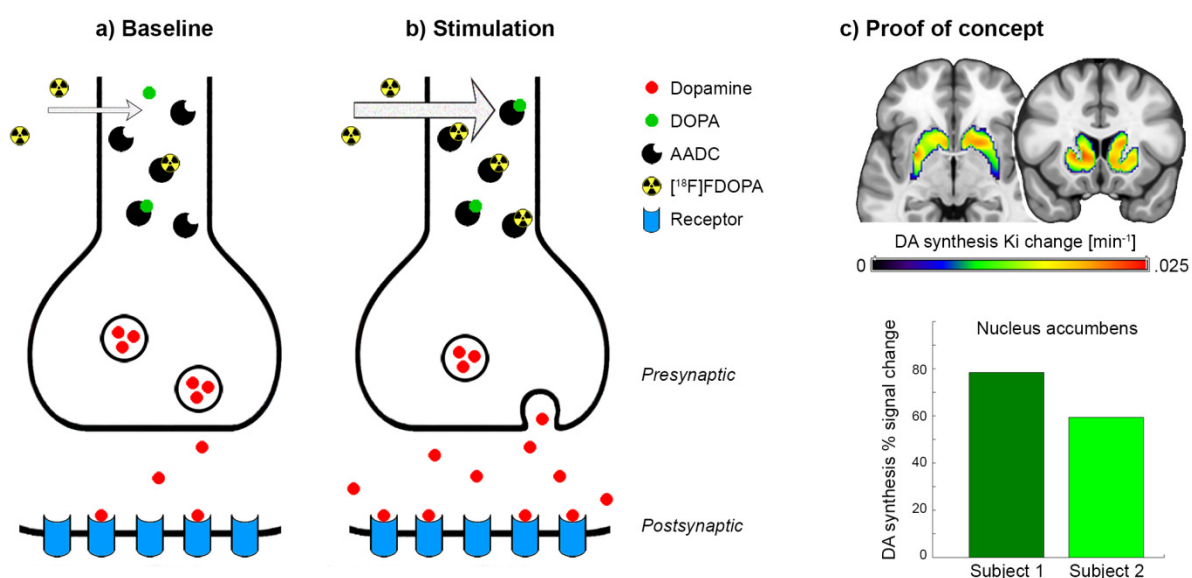


Figure 1: *Synthesis model*. **a)** The neurotransmitter dopamine (DA) is synthesized from its precursor dihydroxyphenylalanine (DOPA) by the enzyme aromatic amino acid decarboxylase (AADC). Use of the radioligand 6-[<sup>18</sup>F]FDOPA as substrate for AADC is a well-established approach to obtain dopamine synthesis rates at baseline. **b)** Neuronal stimulation leads to dopamine release, but also increases AADC activity to refill synaptic vesicles with *de novo* synthesized neurotransmitter, which in turn is reflected in higher radioligand uptake as indicated by arrow thickness. **c)** The proof of concept experiment showed a marked increase in dopamine synthesis rates Ki in the nucleus accumbens of 78.4% and 59.4% signal change from baseline for two subjects during performance of the monetary incentive delay task.

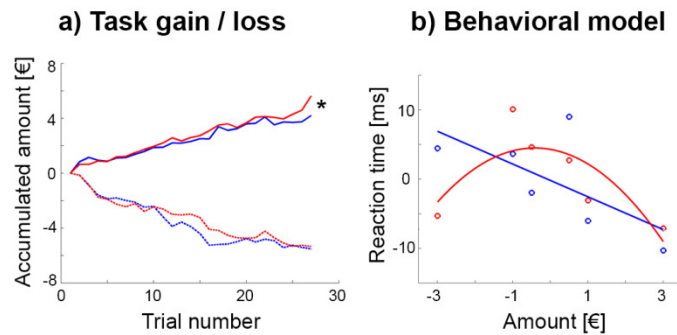


Figure 2: *Behavioral data (blue = men, red = women).* **a)** The monetary incentive delay task was manipulated by modifying the reaction time limit for a successful trial completion, which enabled separate assessment of monetary gain and loss. During the gain task block women earned significantly more money than men ( $5.63 \pm 2.40$  € vs.  $4.21 \pm 1.67$  €,  $t = 2.1$ ,  $*p = 0.047$ ), but both groups showed similar loss ( $-5.33 \pm 1.85$  € vs.  $-5.51 \pm 1.86$  €,  $p = 0.8$ ). **b)** The association between the individually normalized reaction times and the gained/lost amount of money was modelled by a linear relationship in men (reaction time =  $-0.18 - 2.36 \cdot \text{amount}$ ,  $p_{\text{linear}} = 0.0012$ ,  $p_{\text{quadratic}} = 0.11$ ), where a steeper negative slope indicated faster reaction time and thus higher sensitivity for reward. In contrast, the association was characterized by an inverted u-shaped function in women (reaction time =  $4.31 - 0.95 \cdot \text{amount} - 1.16 \cdot \text{amount}^2$ ,  $p_{\text{linear}} = 0.2$ ,  $p_{\text{quadratic}} = 0.001$ ). Since these two functions exhibit the most pronounced difference for high amounts of loss, a strong negative quadratic term was interpreted as high sensitivity for punishment. Circles denote average values, lines are model fits across the entire data set ( $n = 36$  subjects).

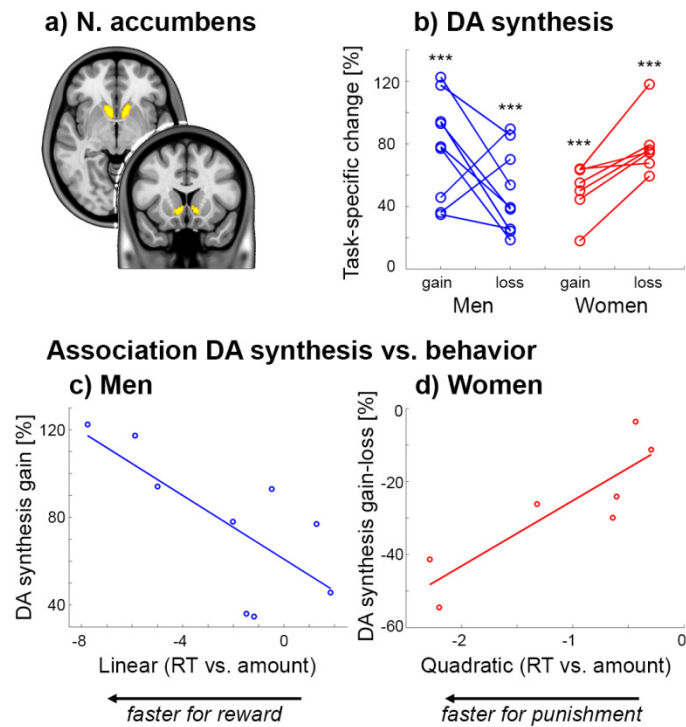


Figure 3: *Functional PET imaging of task-specific dopamine synthesis.* **a)** Region of interest of the nucleus accumbens (NAcc) from the Harvard-Oxford atlas. **b)** Processing of monetary gain and loss resulted in pronounced changes in NAcc dopamine synthesis (\*\**p*<0.001). While men showed higher dopamine synthesis changes for gain vs. loss (*n* = 9), women exhibited the opposite pattern (*n* = 7, see figure 4a). **c-d)** The individually modelled associations between reaction time (RT) and amount were used as indices for reward and punishment sensitivity in men (linear term) and women (quadratic term), respectively (see figure 2b). These behavioral indices showed an association with task-specific changes in NAcc dopamine synthesis during monetary gain in men (c)  $\rho = -0.7$ ,  $p = 0.043$ ) and the difference between gain and loss in women (d)  $\rho = 0.89$ ,  $p = 0.012$ ).

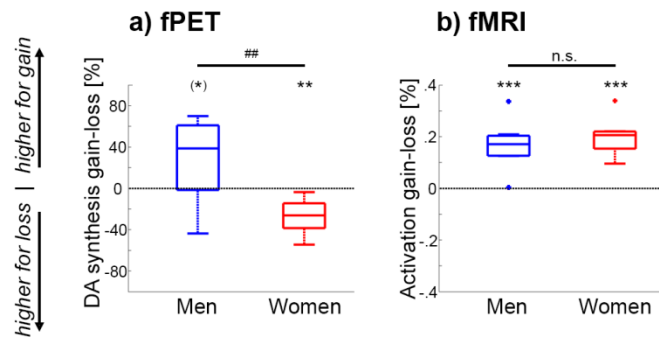
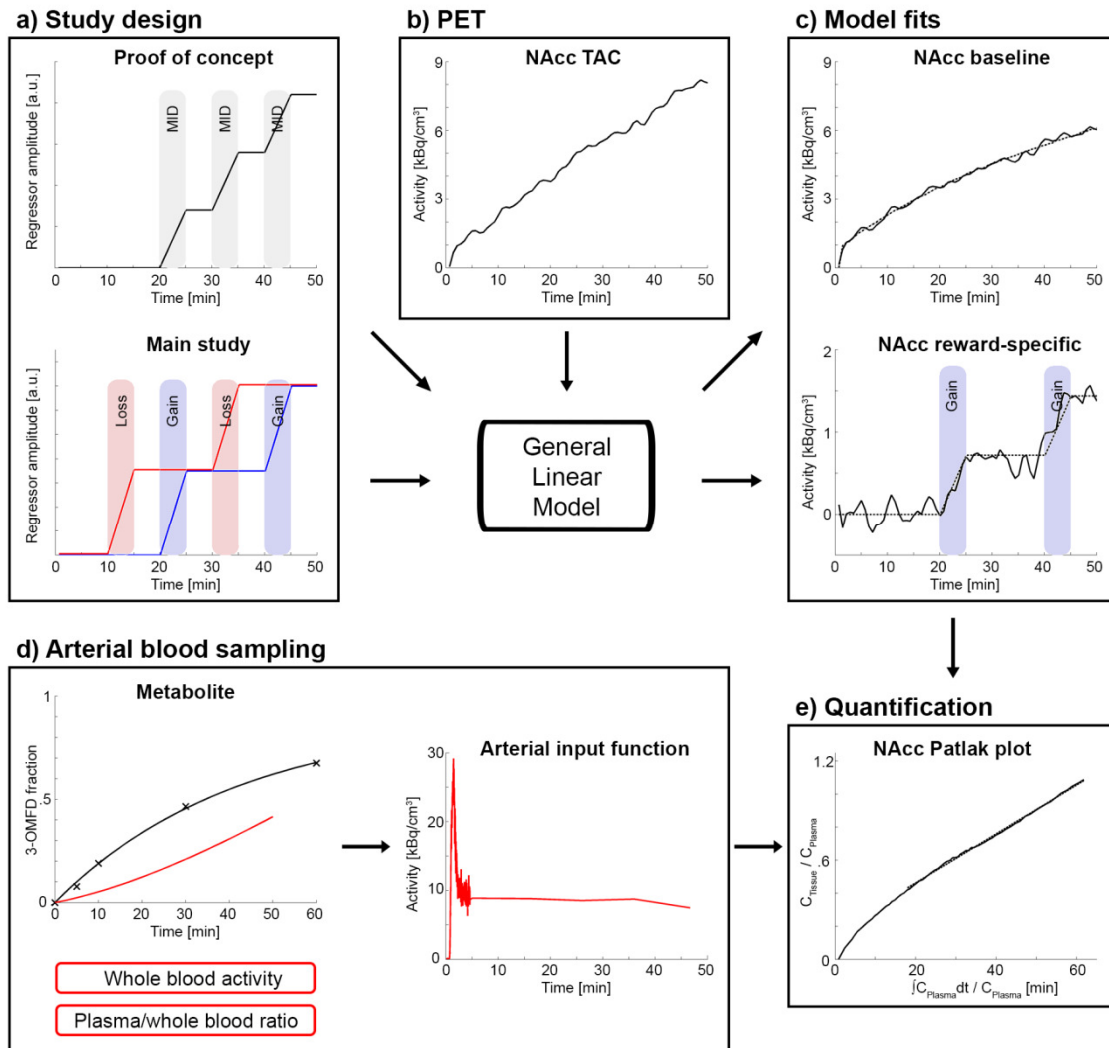


Figure 4: *Comparison between fPET and fMRI.* **a)** In men the task-specific changes in NAcc dopamine synthesis were higher for gain than for loss ( $(^*)p = 0.08$ ). In contrast, women showed the opposite pattern with higher changes in dopamine synthesis during loss vs. gain ( $(^{**})p < 0.01$ ), leading to a significant difference between the two groups ( $t = 3.2$ ,  $(^{##})p = 0.006$ ). **b)** Although neuronal activation obtained with BOLD fMRI indeed showed robust NAcc signal changes for the contrast gain vs. loss for men and women ( $t = 5.5$  to  $6.9$ ,  $(^{***})p = 0.0005$  to  $0.0006$ ), this was not significantly different between the two groups ( $p = 0.4$ ).



Supplementary figure S1: *fPET analysis workflow*. **a)** During the PET scan the monetary incentive delay (MID) task was carried out in blocks of 5 min. In the proof of concept experiment 3 blocks were employed without a separation of gain and loss conditions and an average probability for success of 0.5. For the main study 4 blocks were completed and the MID task was manipulated to disentangle gain and loss by increasing (decreasing) the probability for success (failure) within the corresponding blocks. **b)** PET measurements were carried out using the radioligand 6-[<sup>18</sup>F]FDOPA. The bolus + infusion protocol emphasized the irreversibly uptake of the radioligand. **c)** Time activity curves (TAC) were then modeled according to the design to separate baseline and task-specific effects. Model fits (dotted line) indicate a robust increase in radioligand uptake during the task condition in the nucleus accumbens (NAcc). **d)** The metabolite fraction (3-OMFD) was extracted from previous



studies [50, 51], fitted with a single exponential function (black line) and adapted to match the bolus + infusion protocol (red line). This was combined with the individually measured whole blood activity and plasma to whole blood ratio to obtain the arterial input function, which reaches steady state approximately after 5 min. **e)** Quantification was carried out with the Patlak plot, yielding dopamine synthesis rates at baseline and for each task condition. All data for the TAC (b), model fits (c), arterial input function (d) and quantification (e) were extracted from a representative subject.